Mem. S.A.It. Vol. 83, 643

Memorie della

The multi-frequency properties of AE Aquarii and its evolution from a high mass transfer history

P. J. Meintjes, B. Oruru, and A. Odendaal

Department of Physics, University of the Free State, Po Box 339, Bloemfontein, 9300, South Africa: e-mail: MeintjPJ@ufs.ac.za

Abstract. The multi-frequency properties of the novalike variable AE Aquarii has been reviewed within the framework of its secular evolution and a very effective magnetospheric propeller process. It has been shown that a run-away thermal mass transfer occurred, exceeding $\dot{M}_2 \geq 10^{19}$ g s^{-1}, between 2.7 $\geq$ q $\geq$ 0.73. This resulted in the presence of an accretion disc spinning the white dwarf up to a very short period of $\sim$ 33 s. Thermal time scale mass transfer for q $\leq$ 0.73 decreased to $\dot{M}_2 \sim 10^{17}$ g s^{-1}, which is propelled out of the system by the fast rotating magnetosphere. The very peculiar broad band emission from radio to possibly TeV gamma-rays is a manifestation of the propeller driven spin-down power of the white dwarf, which is $L_{\rm prop} \sim 10^{34}$ erg s^{-1}. This may put AE Aquarii in the class of rotation-powered pulsars, and provide an attractive framework to explain the earlier reports of the transient VHE-TeV gamma-ray emission.

Key words. binaries: cataclysmic variables: radiation mechanisms: non-thermal – pulsars: individual: AE Aquarii – X-rays

1. Introduction

The novalike variable AE Aquarii is probably one of the best studied sources in the sky, from radio to TeV gamma-rays (Meintjes & de Jager 2000). The system consists of a $(0.8 - 0.9)M_{\odot}$ fast rotating $P_{\rm rot} \approx 33$ s white dwarf orbiting a $(0.5 - 0.6)M_{\odot}$ K3-5 secondary star every 9.88 hours (Patterson 1979). The secondary star appears to be overluminous for its mass (Patterson 1979), possibly an attribute of being evolved. Another peculiar aspect of the system is the abnormal line ratios observed from UV data, indicating N V and Si IV abundances that are approximately 10 times higher than He II and C IV (Jameson, King and Sherrington 1980; Mauche, Lee & Kallman 1997), possibly being an indication of CNO cycling in the convective envelope reaching down to deep within the stellar interior (Schenker et al. 2002). This may further support the notion of an evolved secondary star, perhaps being stripped of its outer envelope during a violent mass transfer history.

The system displays erratic optical flaring which results in the apparent magnitude ranging between $m_{\rm v} \approx 10$(flares) – 12(quiescence), indicated in Fig. 1. The rotation period of the white dwarf manifests as a low amplitude (0.1 – 0.2)% 33.08 s modulation superimposed on the optical light curve, which in a FFT, re-

Send offprint requests to: P.J. Meintjes

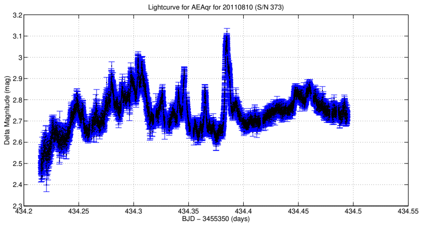

Fig. 1. Optical lightcurve of AE Aquarii showing rapid intensity variations. The observation was made recently with the UFS-Boyden Observatory's 1.5 m telescope outside Bloemfontein (SA).

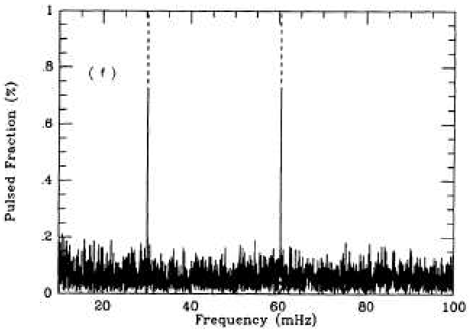

Fig. 2. Optical FFT power spectrum during quiescence and flares. In quiescence the spin period of $P_* \sim 33.08$s and its first harmonic correspond to peaks at $(\nu_f; 2\nu_f) = (30.23; 60.46)$ mHz (adopted from Meintjes et al. 1994).

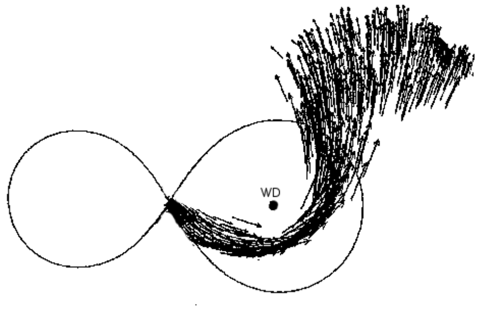

Fig. 3. Illustrating the propeller process in AE Aquarii (adopted from Wynn, King & Horne 1997).

veals maximum power at $\nu_* = 30.23$ mHz and its first harmonic (e.g Fig. 2). It has been shown (de Jager et al. 1994) that the white dwarf is spinning down at a rate of $\dot{P} = 5.6 \times 10^{-14}$ s s^{-1}, consistent with the spin-down found in a more recent study (Mauche 2006). This spin-down implies an inferred spin-down power of $P_{sd} = I\Omega\dot{\Omega} \sim 10^{34}$ erg s^{-1}, which is approximately 500 times higher (e.g. Meintjes & de Jager 2000) than the observed accretion induced luminosity, i.e. $L_{acc} \sim 2 \times 10^{31}$ erg s^{-1}, derived from *HST* ultra-violet (UV) and X-ray data (Eracleous, Halpern & Patterson 1991; Eracleous & Horne 1996). The fast rotating magnetosphere results in AE Aquarii being in a propeller phase, expelling the majority of the mass transfer flow from the binary system (e.g Fig. 3) (e.g. Wynn, King & Horne 1997; Meintjes & de Jager 2000).

The propeller ejection of matter from the system is probably the driving mechanism behind all the non-thermal emission from radio to the reported, but unconfirmed, VHE ($\epsilon_\gamma \geq$ 350 GeV) and TeV ($\epsilon_\gamma \geq 1000$ GeV) gamma-rays. The reported TeV gamma-ray emission showed pulsations corresponding to the 33 s rotation period of the white dwarf, as well as short minute time-scale bursts (Meintjes et al. 1992,1994; Chadwick et al. 1995). The derived duty cycle for the burst-like emission was approximately $\delta_{burst} \sim 0.024\%$, while the duty cycle for strong pulsed emission close to the spin period of the white dwarf, above the 99.999 % confidence level, was $\delta_{pulsed} \sim 1\%$. However, weak pulsed emission at the spin period, above the 95 % significance level, was detected more often with a duty cycle of approximately $\delta_{weak} \sim 30\%$ in all the observations between 1988-1991 (Meintjes et al. 1992, 1994). The Spectral Energy Distribution (SED) of AE Aquarii (Fig. 4) showing the total emission from radio to TeV gamma-rays has been constructed (e.g. Dubus et al. 2004 (and references therein), Terada et al. 2008, Chadwick et al. 1995 (VHE), Meintjes et al. 1992, 1994 (TeV)).

2. Secular evolution of AE Aquarii

The time evolution of the orbit, i.e. $(\dot{a}/a)$, is given by

$$\frac{\dot{a}}{a} = 2\frac{\dot{J}_{orb}}{J_{orb}} + \frac{\dot{M}}{M} - 2\frac{\dot{M}_1}{M_1} - 2\frac{\dot{M}_2}{M_2}, \quad (1)$$

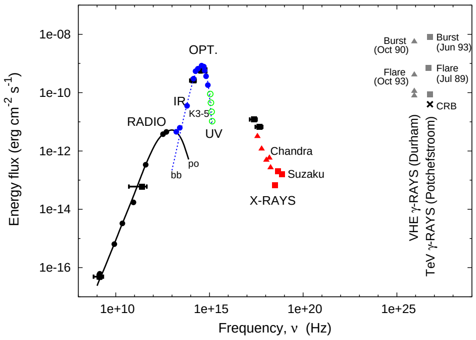

Fig. 4. The SED of AE Aqr from radio to the reported, but unconfirmed, TeV gamma-rays.

which depends on the rate of change of the orbital angular momentum ($\dot{J}_{\rm orb}/J_{\rm orb}$), the mass loss from the system ($\dot{M}/M$), mass accretion by the primary star ($\dot{M}_1/M_1$) and the mass transfer rate ($\dot{M}_2/M_2$) from the secondary star (e.g. Wynn & King 1995).

If a fraction (η) of the angular momentum crossing the L1 region is lost from the binary (e.g. King 1993; Wynn & King 1995), the angular momentum losses are approximated by

$$\frac{\dot{J}_{\rm orb}}{J_{\rm orb}} = \eta\frac{\dot{J}_{\rm ov}}{J_{\rm orb}} = \eta\dot{M}_2\frac{(GM_1R_{\rm circ})^{1/2}}{J_{\rm orb}}. \quad (2)$$

It can be shown that the mass loss and the mass accreted by the white dwarf are related through

$$\dot{M} = \alpha\dot{M}_2 \;\;:\;\; \dot{M}_1 = -(1-\alpha)\dot{M}_2 = -\beta\dot{M}_2 \quad (3)$$

where α represents the fraction of the Roche lobe overflow escaping from the system, and where $\beta = (1-\alpha)$ represents the fraction of the mass transfer accreted by the compact star. The negative sign indicates positive accretion since it is assumed both $\dot{M}$ and $\dot{M}_2$ are negative quantities.

The current properties of AE Aquarii is consistent with a high mass accretion history (Schenker et al. 2002; Meintjes 2002). If one consider initial parameters $P_{\rm orb,i} \sim 15$h, $M_{1,i} \sim 0.6M_\odot$, $M_{2,\rm i} \sim 1.6M_\odot$ (i.e. $q_{\rm i} \sim 2.7$) and $R_2 \sim 1.6R_\odot$, it can be shown that the initial thermal time scale ($\tau_{\rm th} \sim 6.3\times10^6(M_2/1.6M_\odot)^{-1}$ yr) mass transfer could have been of the order

$$\dot{M}_{2,\rm i} \sim 2\times10^{19}(M_{2,\rm i}/1.6\,M_\odot)(\tau/\tau_{\rm th})^{-1}\ {\rm g\ s^{-1}}, \quad (4)$$

still below the Eddington value of $\dot{M}_{\rm Edd} \leq 7\times10^{20}(M_{1,\rm i}/0.6\,M_\odot)^{-0.8}$ g s^{-1}.

It can be shown that for non-conservative binary evolution, using $(\alpha,\beta) \sim 0.5$ and $\eta \sim 0.1$, the binary shrinks down into the photosphere of the secondary star at a rate $\dot{a}_{\rm ev} \sim -0.002$ cm s^{-1}. This results in the orbit decreasing a distance equal to a stellar scale height $H_* \sim 3\times10^7(T_*/6500\,{\rm K})$ cm on a time scale

$$\Delta\tau \sim 500\left(\frac{\Delta a}{H_*}\right)\left(\frac{\dot{a}}{\dot{a}_{\rm ev}}\right)^{-1}\ {\rm yr}, \quad (5)$$

which is several orders of magnitude smaller than the thermal time scale. This may have been a trigger mechanism for a run-away mass transfer process if the Roche lobe radius decreased more than one stellar scale height. It has been shown that this could have lasted until a critical q-ratio was reached, i.e. $q_{\rm crit} = 0.73$ (Meintjes 2002). It has been shown that accretion disc torques could spin-up the white dwarf to periods around ~ 30 s over a time scale $\tau_{\rm su} \sim 3\times10^6$ yr, which is similar to the thermal mass transfer time scale, i.e. $\tau_{\rm mt} \sim$ few$\times10^6$ yr (Meintjes 2002). A mass accretion rate scenario where $\beta \sim 0.5$ of the thermal time scale mass transfer rate, is sufficient to drive thermal nuclear burning on the surface of the white dwarf, which is of the order (Prialnik 1986)

$$\dot{M}_{1,\rm i} \geq 5\times10^{18}\left(\frac{M_{1,\rm i}}{0.6\,M_\odot}\right)^{3/2}\ {\rm g\ s^{-1}}. \quad (6)$$

Therefore, during this run-away mass transfer phase AE Aquarii could have been a Super Soft X-ray Source (SSS). The subsequent thermal mass transfer rate from $q \leq q_{\rm crit}$ is at a much more modest rate, i.e. $\dot{M}_2 \sim 3\times10^{17}$ g s^{-1}, resulting in the highly spun-up white dwarf propelling the mass flow from the system. This results in the white dwarf occupying a spin-down phase for the past $\tau_{\rm sd} = \tau_{\rm th} \sim 10^7$ yr (de Jager et al. 1994. Meintjes & de Jager 2000).

3. Magnetospheric propeller

It can be shown that the current thermal time scale mass transfer rate from the secondary star is

$$\dot{M}_2 \sim 4 \times 10^{17} \left(\frac{M_2}{0.6\,M_\odot}\right)\left(\frac{\tau_{\rm th}}{10^7\,{\rm yr}}\right)^{-1} \ {\rm g\ s^{-1}}. \quad (7)$$

If this is representative of the accretion rate, it would drive an accretion luminosity $\sim$ few $\times$ $10^3\,L_{\rm acc}$. The weak $\sim (0.1 - 0.2)\%$ modulation of the 33 s pulsed signal suggests that the bulk of the mass transfer flow is not converted to heat and radiation on the surface of the white dwarf. Possible MHD propellering may occur at the the magnetospheric radius (Alfvén radius), where the field starts to dominate the mass flow dynamics. This is of the order

$$R_{\rm M} = 10^{10}\left(\frac{M_*}{0.9\,M_\odot}\right)^{-1/7}\left(\frac{\dot{M}_{2,17}}{4}\right)^{-\frac{2}{7}} \mu_{33}^{\frac{4}{7}}\ {\rm cm}, \quad (8)$$

where μ_{33} is the magnetic moment of the WD in the units of 10^{33} G cm^3 and $\dot{M}_{2,17}$ represents the mass transfer rate in units of 10^{17} g s^{-1}. At the Alfvén radius, the magnetosphere rotates with a velocity

$$v_{\rm rot} \simeq 2 \times 10^9 (\frac{M_*}{M_\odot})^{-1/7} \dot{M}_{17}^{-\frac{2}{7}} P_{33}^{-1} \mu_{33}^{\frac{4}{7}}\ {\rm cm\ s^{-1}}. \quad (9)$$

The Keplerian velocity of the orbiting matter at this radius is

$$v_{\rm K} \simeq 10^8 \left(\frac{M_*}{M_\odot}\right)^{4/7} \dot{M}_{17}^{1/7} \mu_{33}^{-\frac{2}{7}}\ {\rm cm\ s^{-1}}. \quad (10)$$

For $\dot{M} \lesssim 10^{17}$ g s^{-1}, $v_{\rm rot} > v_{\rm K}$ as shown in Figure 5. The high rotational velocity of the magnetosphere with respect to orbiting gas supports the centrifugal expulsion of material from the binary system.

The propeller driven outflow is evident from the width of the Balmer H_α line (e.g. Fig. 6), showing a velocity dispersion that is not compatible with thermal broadening of a $10^4 - 10^5$ K thermal plasma.

The expected velocity dispersion due to thermal broadening of a line emitting gas at temperature $T \sim$ few $\times$ 10^4 K is approximately $\Delta v \leq 30(T/10^4\,{\rm K})^{1/2}$ km s^{-1}, orders less than the observed velocity dispersion visible in the H_α line, which is of the order of $\Delta v \sim 2000$ km s^{-1} (Fig. 7). This can satisfactorily be explained in terms of high velocity

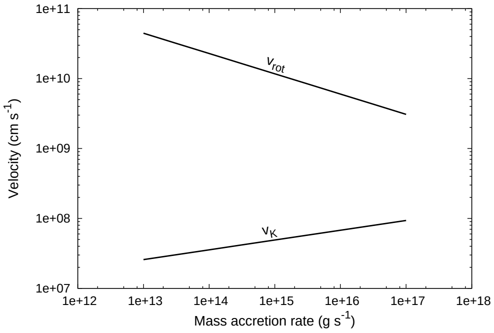

Fig. 5. A comparison between the rotational velocity of the magnetosphere and the Keplerian velocity of the gas at the magnetospheric boundary.

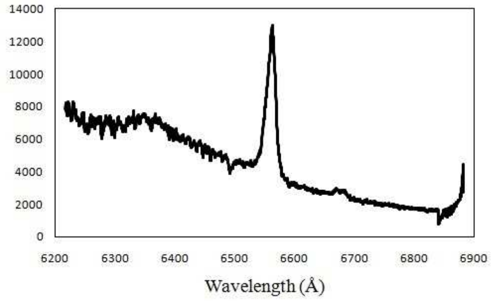

Fig. 6. Optical spectrum obtained with the grating spectrograph on the SAAO 1.9 m telescope during September 2011. The spectrum displays a broad H_α line at 656 nm.

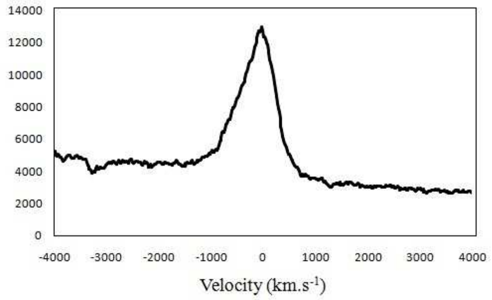

Fig. 7. The velocity dispersion visible in the H_α line.

gas being propelled out of the system due to a magnetospheric propeller process.

If the mass transfer flow is converted to radiation in the propeller zone, the resultant luminosity (in units of 10^{33} erg s^{-1}) is

$$L_{\rm mag,33} \sim 5(\frac{M_1}{0.9M_\odot})(\frac{\dot{M}_{2,17}}{4})(\frac{R}{R_{\rm mag}})^{-1} \qquad (11)$$

for the current thermal time scale mass transfer rate. This is sufficient to drive optical emission associated with flares. Observations seem to suggest that the accretion luminosity inferred from UV - X-ray data is approximately $L_{\rm acc} \sim 10^{31}$ erg s^{-1}, which implies an accretion rate of

$$\dot{M}_* \sim 10^{14} (\frac{L}{L_{\rm acc}})(\frac{R_*}{10^9\,{\rm cm}})(\frac{M_*}{0.9M_\odot})^{-1} {\rm g\ s}^{-1}, \qquad (12)$$

significantly lower than the inferred mass transfer rate. This suggests that the majority of the mass flow from the secondary star is ejected from the binary system. The total MHD power transmitted to the orbiting gas stream is of the order (Meintjes & Venter 2005)

$$\begin{aligned} P_{\rm mhd} \;\approx\; & 10^{34}\left(\frac{v_{\rm rel,\perp}}{2{\times}10^9\,{\rm cm\ s^{-1}}}\right)\left(\frac{B_{\rm circ}}{300\,{\rm G}}\right)^2 \\ & \left(\frac{A_{\rm stream}}{5{\times}10^{20}\,{\rm cm^2}}\right)\ {\rm erg\ s^{-1}}. \end{aligned} \qquad (13)$$

The dissipated magnetospheric power is consistent with the spin-down power of the white dwarf inferred from the spin-down rate (de Jager et al. 1994; Mauche 2006), exceeding the accretion luminosity by several orders of magnitude, i.e. $P_{\rm sd} \sim 10^3 L_{\rm acc}$. The spin-down power provides a huge reservoir of energy that may be channeled into particle acceleration and non-thermal emission (e.g. de Jager 1994; Meintjes & de Jager 2000). A recent study of the X-ray emission from AE Aquarii (Terada et al. 2008) using the Suzaku satellite, showed indications of a non-thermal pulsed hard X-ray component, a tell-tale signature of particle acceleration in the system.

4. Particle acceleration and non-thermal emission

The non-thermal nature of the hard X-ray emission in AE Aquarii and the continuous non-thermal flaring below $\nu \leq 10^{13}$ Hz (e.g. Dubus et al 2004) provide evidence that a fraction of the spin-down power may be converted into particle acceleration through different mechanisms.

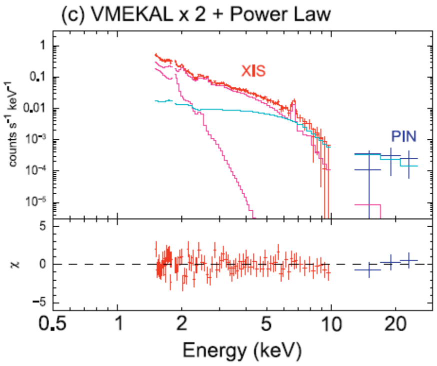

Fig. 8. The soft and hard X-ray spectrum observed by Suzaku. Noticeable is a possible power-law hard X-ray component above 10 keV (Adopted from Terada et al. 2008).

4.1. Non-thermal radio - IR flares

The highly transient non-thermal emission in AE Aquarii can be satisfactorily explained within the framework of the interaction between the magnetospheric propeller and magnetized blobs in the mass transfer stream. It can be shown that a fast moving magnetic disturbance propagating through a gas with the Alfvén velocity $\mathbf{v}_{\rm A}$, can transfer energy to thermal electrons moving with a velocity $\mathbf{v}_{\rm e}$ in the frozen-in fields, i.e.

$$\begin{aligned} \frac{d\epsilon_{\rm e}}{dt} &= (-e/c)\mathbf{v}_{\rm A}.(\mathbf{v}_e \times \mathbf{B}) \\ &= \mathbf{v}_{\rm A}.\mathbf{F}_{\rm L}. \end{aligned} \qquad (14)$$

These electrons will experience a push from the Lorentz force, resulting in a sudden increase in energy. For thermal velocities of the order of the sound speed $v_{\rm e} \sim 3 \times 10^6 (T_{\rm blob}/10^5\,{\rm K})^{1/2} {\rm cm\ s}^{-1}$, and an Alfvén velocity of the order of $v_{\rm A} \sim 4 \times 10^6 (B_{\rm blob}/300\,{\rm G})(\rho/\langle\rho_{\rm bstream}\rangle)^{-1/2}\ {\rm cm\ s}^{-1}$, the rate at which energy is being transferred to thermal electrons in magnetized blobs is

$$\frac{d\epsilon_{\rm e}}{dt} \approx 40\left(\frac{T_{\rm surf}}{10^5\,{\rm K}}\right)\left(\frac{B}{300\,{\rm G}}\right)\ {\rm MeV\ s^{-1}}. \qquad (15)$$

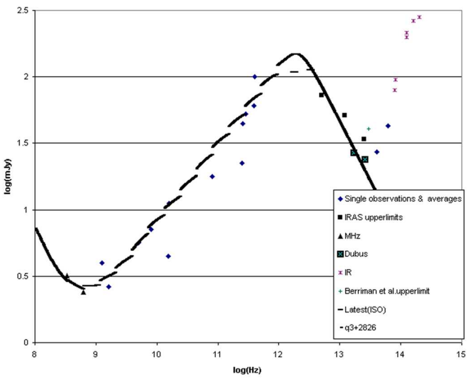

Fig. 9. The non-thermal emission from expanding synchrotron emitting clouds from radio to IR frequencies (adopted from Venter & Meintjes 2006).

This mechanism can accelerate electrons in magnetized blobs to energies reaching at least $\gamma_e \sim 250$ ($\epsilon_e \sim 130$ MeV) within the dominant energy loss time scales, explaining the radio-IR synchrotron emission from expanding magnetized blobs (shown in Figures 4 and 9). Also visible from Figure 9 is the prediction of a radio remnant below 1 GHz (Venter Meintjes 2006).

4.2. High energy emission

The recent Suzaku observations reveal a pulsed hard X-ray component $\epsilon_X \geq 10$ keV, with a photon power law index of $\Gamma = 1.16$, compatible with the photon power law index $\Gamma \sim 1.4$ of young rotation-powered pulsars (Gotthelf 2003). Similarly, the rapid spin-down of the white dwarf in the current low mass accretion phase puts AE Aquarii in the class of rotation-powered pulsars. The spin-down may be instrumental in driving huge electric fields along the magnetic field lines. The electric field component parallel to the magnetic field, $E_{\|}$, is (Arons & Scharlemann 1979; Ikhsanov & Bierman 2006):

$$E_{\|} = E^{\|}_{\rm AS}\sqrt{2R/r}, \tag{16}$$

where

$$E^{\|}_{\rm AS} = \frac{1}{8\sqrt{3}}\left(\frac{\Omega_* R}{c}\right)^{5/2} B_*. \tag{17}$$

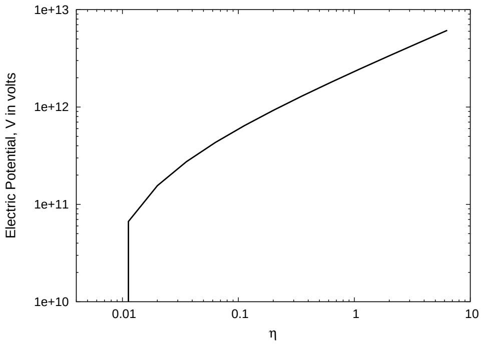

Fig. 10. Electric field potential (V) as a function of radius ($\eta = r/R_{\rm lc}$).

It can be shown that

$$E^{\|}_{\rm AS} \simeq 10^4\, P_{33}^{-\frac{5}{2}}\mu_{33}R_9^{-1/2}\ {\rm V\ m^{-1}}, \tag{18}$$

which translates to

$$E_{\|} \simeq 10^3 P_{33}^{-\frac{5}{2}}\mu_{33} r_{l,11}^{-1/2}\ {\rm V\ m^{-1}}, \tag{19}$$

in the vicinity of the light cylinder radius.

The electric potential in the region of the polar cap is

$$\begin{aligned} V_{\rm pc}(r) &= \int_R^r E_{\|} ds \\ &\simeq 2\times 10^{11} P_{33}^{-\frac{5}{2}}\mu_{33}R_9^{1/2}\left[\left(\frac{r}{R}\right)^{1/2} - 1\right]\ {\rm V}. \end{aligned} \tag{20}$$

Close to the light cylinder, ($R_{\rm lc} \simeq c/\Omega_*$), the potential is

$$V(R_{\rm lc}) \simeq 3\times 10^{12} P_{33}^{-2}\mu_{33}\ {\rm V}. \tag{21}$$

Figure 10 shows the variation of electric potential with distance from the white dwarf, normalized with respect to the light cylinder radius ($\eta = r/R_{\rm lc}$), which is of the order of $R_{\rm lc} \approx 5$ ls (ls = light seconds). Close to the surface of the WD, the potential difference is zero ($V = 0$), increasing to values of the order of 1 Tera Volt at the cylinder radius and beyond.

Line emission profiles observed during *HST* observations are consistent with interblob plasma densities in the propeller zone ($R_{\rm prop} \geq 10^{10}$ cm) (Wynn, King & Horne 1997) between $n_{\rm p} \sim 10^6 - 10^{11}\ {\rm cm^{-3}}$ (Eracleous & Horne 1996), with an adopted median value of $n_{\rm p} \sim$

$10^{10}\,\mathrm{cm}^{-3}$. The low accretion rate, compared to the mass transfer rate, i.e. $\kappa = (\dot{M}_1/\dot{M}_2) \sim 10^{-3}$, may imply that the plasma density closer to the white dwarf ($r < R_{\rm prop}$) may reach values close to the so-called Goldreich-Julian density (Goldreich & Julian 1969), which is

$$n_{\rm GJ} \simeq 2\times 10^3\, B_{*,6} P_{33}^{-1}\ \mathrm{cm}^{-3}, \tag{22}$$

where $B_{*,6}$ is the surface field strength of the WD in the units of 10^6 G. In such low density plasmas electric fields can be sustained without being shorted out by electrostatic shielding. The effective acceleration of electrons will be determined by ionization losses in the plasma and the synchrotron losses.

The mean free path of thermal electrons in a plasma with density $n_{\rm p}$ is $\lambda_{\rm e} = (1/n_{\rm p})(1/\ln\Lambda)(\pi e^2/8\epsilon_\circ E_{\rm e})^{-2}$, with $\ln\Lambda$ representing the Coulomb logarithm, ranging between $\ln\Lambda \sim 10 - 20$ (e.g. Terada et al. 2008). Then it can be shown that thermal electrons with energy $E_{\rm th} \sim 1\,\mathrm{keV}$ in the plasma density range given above, have mean free paths ranging between $\lambda_{\rm e} \sim 10^6(n_{\rm p}/10^{11}\,\mathrm{cm}^{-3})^{-1}\,\mathrm{cm} - 10^{11}(n_{\rm p}/10^6\,\mathrm{cm}^{-3})^{-1}\,\mathrm{cm}$. One can also show that a thermal plasma exposed to an electric field in excess of the so-called Dreicer field, $E_{\rm D} \sim 2\times 10^{-10}\,(n_{\rm e}/T_{\rm eff})\,\mathrm{statvolts\,cm}^{-1}$ (e.g Meintjes & de Jager 2000 and references therein), will accelerate freely without experiencing the inhibiting effect of particle-particle collisions. For AE Aquarii, the upper limit to the Dreicer field is of the order of

$$E_{\rm D} \leq 0.1 n_{e,11} T_{\rm eff,7}^{-1}\ \mathrm{V\,m}^{-1}, \tag{23}$$

where the particle density and temperature are expressed in units of $10^{11}\,\mathrm{cm}^{-3}$ and 10^7 K respectively. One can see that $\delta = \frac{E_{\parallel}}{E_D} \geq 10^4$, for the typical values mentioned above, implying the effective acceleration of the electron population as a whole.

It can be shown that synchrotron losses in the magnetosphere, inside the propeller zone, limit electron energies to

$$\gamma_{\rm e} = 10^5 \left(\frac{R_{\rm prop}}{10^{10}\,\mathrm{cm}}\right)^{-1} \left(\frac{B_{\rm p}}{130\,\mathrm{G}}\right)^{-2} \tag{24}$$

where $B_{\rm p}$ is the value of the magnetospheric field in the propeller zone. The frequency at which individual electrons with energies $\gamma \sim 10^5$ radiate most of their energy, is then

$$\nu_{\rm c} = 5\times 10^{18} \left(\frac{B_{\rm p}}{130\,\mathrm{G}}\right)\left(\frac{\gamma_{\rm e}}{10^5}\right)^2\ \mathrm{Hz}, \tag{25}$$

consistent with the hard X-ray emission detected with the Suzaku satellite (Figure 4) reported by Terada et al. (2008). The reported hard X-ray luminosity of $L_{\rm x} \sim 5\times 10^{29}\,\mathrm{erg\,s}^{-1}$ (Terada et al. 2008) corresponds to 0.01% of the spin-down power, putting AE Aquarii in the same category as young rotation-powered pulsars in the 2-10 keV energy range (Becker & Trumpher 1997).

Highly relativistic electrons with energies $\gamma \sim 10^5$ provide an interesting possibility for high energy gamma-ray production by upscattering optical photons ($\epsilon_{\rm ph} \sim 1$ eV) from the K-type companion star, or propeller ejected outflow, to high energies, i.e. the inverse Compton process. It can be shown that the inverse Compton process occurs in the Thomson limit for photon frequencies

$$\nu < 1.2\times 10^{15}\left(\frac{\gamma}{10^5}\right)^{-1}\ \mathrm{Hz}, \tag{26}$$

which is consistent with the optical photons from the K3-5 secondary star (Figure 4). An upper-limit for gamma-ray energies produced in the Thomson limit is

$$\epsilon_\gamma \leq 0.2\left(\frac{\gamma}{10^5}\right)^2\left(\frac{\epsilon_{\rm ph}}{5\,\mathrm{eV}}\right)\ \mathrm{TeV}, \tag{27}$$

which provides an interesting prospect for follow-up studies using *Fermi* and modern Cerenkov facilities.

It has been shown (Meintjes & de Jager 2000) that the burst-like VHE and TeV gamma-ray emission (Meintjes et al. 1992, 1994; Chadwick et al. 1995) is consistent with proton acceleration and gamma-ray production through π° decay in the circumbinary ring of propeller ejected gas. Since protons do not suffer synchrotron losses, the proton energies can indeed significantly exceed the electron energies. The low duty cycle of the reported emission, require dedicated follow-up campaigns with, among others, *HESS*, to verify the possible VHE and TeV gamma-ray status of this enigmatic source.

5. Conclusions

In this paper the peculiar properties of AE Aquarii have been presented within the theoretical framework of its evolution from a possible SSS history and a current propeller phase. It has been shown that a run-away mass transfer phase $\sim 10^7$y ago may have spun the white dwarf up to ~ 33 s. The mass transfer and accretion rates could have been $\dot{M}_1 \geq 10^{19}$ g s^{-1}, enough to drive nuclear burning on the white dwarf surface. A subsequent decrease in mass transfer for $q \leq 0.73$ resulted in the spun-up white dwarf propelling the mass flow from the system, with the subsequent production of the unique thermal and non-thermal multi-frequency emission, from radio to possibly TeV gamma-rays.

6. Discussion

ANDREW KING: I agree that it is very likely that AE Aqr have deccended from a supersoft source. Another sign is the C/N ratio indicating that the secondary star must have been more massive in the past. The short evolution time scale of AE Aqr suggests that systems like this might be quite common. Is there any progress in determining what fraction of CVs show signs of abundance anomalies, and so could have descended from this evolutionary route?

CHRISTIAN KNIGGE's Comment: Boris Gansicke and collaborators showed from a UV snapshot survey that there are some clear examples of abundance anomalies pointing to thermal time scale mass transfer evolution, but it is only a handful, probably not a large percentage of the known cv's

Acknowledgements. The author is grateful for the invitation to the Golden Age of CV's and Related Objects workshop in Palermo, Sicily. The author thank Dr. C. Mauche for enlightening discussions related to the X-ray emission of AE Aqr.

References

Arons, J. & Scharlemann, E. T. 1979, ApJ, 231, 854
Becker, W. & Trumpher, J. 1997, A&A, 326, 682
Chadwick, P.M. et al. 1995, Astroparticle Physics, 4, 99
Dubus, G. et al., 2004, MNRAS, 349, 869
de Jager, O. C. 1994, ApJ. Suppl., 90, 775
de Jager, O. C. Meintjes, P. J. O' Donoghue, D. & Robinson, E. L. 1994, MNRAS, 267, 577
Eracleous, M. Halpern, J. & Patterson, J. 1991, ApJ, 382, 290
Eracleous, M. & Horne, K. 1996, ApJ 471, 427
Goldreich P. & Julian W. 1969, ApJ, 175, 869
Gotthelf, E.V. 2003, ApJ, 591, 361
Ikhsanov, N. & Bierman P. L. 2006, A&A, 445, 305
Jameson, R.F., King, A.R. & Sherrington, M.R. 1980, MNRAS, 191, 559
King, A.R. 1993, MNRAS, 261, 144
Mauche, C.W., Lee, Y.P., & Kallman, T.R. 1997, ApJ, 477, 832
Mauche, C., 2006, MNRAS, 369, 1983
Meintjes, P. J. et al. 1992, ApJ, 401, 325
Meintjes, P. J. et al. 1994, ApJ, 434, 292
Meintjes, P. J. & de Jager, O. C. 2000, MNRAS, 311, 611
Meintjes, P. J. 2002, MNRAS, 336, 265
Meintjes, P.J. & Venter, L. A. 2005, MNRAS, 360, 573
Patterson, J. 1979, ApJ, 234, 978
Prialnik, D. 1986, ApJ, 310, 222
Schenker, K. King, A. R. Kolb, U. Wynn, G. A. & Zhang, Z. 2002, MNRAS, 337, 1105
Terada, Y. et al. 2008, Publ. Astron. Soc. Japan, 60, 387
Venter, L.A. & Meintjes, P.J. 2006, MNRAS, 366, 557
Wynn, G.A. King, A.R., 1995, MNRAS, 275, 9
Wynn, G. A. King, A. R. & Horne, K. 1997, MNRAS, 286, 436